Desalination and Water Treatment
www.deswater.com
doi: 10.5004/dwt.2019.24048

154 (2019) 305–311
June

Study on sodium alginate and phosphoric acid modified biomass power plant ash as water treatment biofilm carrier

Feipeng Li[a,*], Wei Liu[a], Yubao Jia[a], Zengsheng Zhang[b], Hong Tao[a], Xiaodong Zhang[a]

[a]*School of Environment and Architecture, University of Shanghai for Science and Technology, Shanghai 200093, China, Tel. +86 (0) 2155275979; emails: leefp@126.com (F. Li), liuweifwk@foxmail.com (W. Liu), jiayubao@163.com (Y. Jia), taohong@usst.edu.cn (H. Tao), zhangxiaodong@usst.edu.cn (X. Zhang)*
[b]*Suzhou SaiHua Instrument Control Limited Company, Suzhou 215151, China, email: tongjizhangzs@163.com*

Received 15 August 2018; Accepted 1 March 2019

ABSTRACT

In this study, we developed a new biofilm carrier by using biomass power plant ash modified by a combination of sodium alginate and phosphoric acid. Specific surface area, pore size distribution, and surface functional groups of this new modified biofilm carrier were characterized by using scanning electron microscopy, water treatment experiments, and 454 pyrosequencing. The results showed that the specific surface area of the modified biomass ash was seven times larger than that of the raw material. The majority of pores were identified as mesoporous. Surface functional groups significantly increased after modification with a certain amount of hydroxyl, carboxylic acid, phosphate, hydrogen phosphate groups, and C–H bond, etc, which can help to attach more microorganisms. The scanning electron microscopy (SEM) showed that the surface of modified material has porous honeycomb structure. Hanging membrane experiment indicated that microbiological membrane could attach to the surface and grow well. The removal efficiency of chemical oxygen demand (COD_{cr}) and NH_3–N in the test water was better than that of the raw materials as a result of biofilm formation, and the removal rate was 67.6% and 65.7%, respectively. Pyrosequencing analysis showed that, in the biofilm carrier, Proteobacteria accounted for the largest portion (77.09%), followed by the Bacteroidetes (7.43%), Acidobacteria (3.99%), and Nitrospirae (3.69%), in accordance with better COD_{cr} and NH_3–N removal effects.

Keywords: Biomass ash; Modification; Characterization; Microbial carrier; Pyrosequencing

1. Introduction

With the increasing consumption of traditional energy and the advancement of new policies, the biomass power industry becomes more important than the previous years. However, a normal biomass power plant that uses forestry and agricultural residues as the main fuel can produce 5%–10% mass ratio of biomass ash during the energy production [1]. Unlike fly ash, biomass power plant ash belongs to the boiler bottom residue. It is the by-product of the combustion of straw, bark and other fuels at 700°C–800°C with both poor structure and chemical-based agglomerate. In addition, there is organic matter in the ash because of incomplete combustion [2]. In the recent years, biomass ash was widely used in, for instance, building materials [3,4], fertilizer, soil improvement [5–7], and chemical extraction [8,9]. However, it is rarely used in water treatment except for studies on its physical and chemical adsorption effects [10–12]. For example, Tian et al. [13] studied the effect of different particle sizes of biomass ash on sewage treatment. Although the removal of pollutants through entrapment and absorption was good in the early stages, with the gradual saturation of absorption sites on the ash surface over time, the treatment effect reduced sharply. The usage of biomass ash depends on its physical

* Corresponding author.

and chemical properties. The application of biomass power plant ash could be increased by modifying its pore structure and surface properties, which is of great significance for the reuse of biomass ash waste.

In water treatment, biofilm carriers are used for fixing biological cells and enzymes onto a bio-membrane. The specific surface area, porosity, and surface functional groups are important factors for the microbial attachment [14,15]. Nowadays, the biofilm carrier materials mainly include inorganic fillers and organic synthetic fillers. Due to large specific gravities, it is difficult to fluidise and recycle inorganic fillers (e.g., sand and zeolite). On the other hand, organic synthetic fillers also have many disadvantages including, weak biological compatibility, low treatment effect, and being difficult for regeneration [16,17]. There are numerous studies on the use of modified fly ash as the adsorption material. In order to increase the surface pores, high concentrations of acid and alkali were used, which is expensive and might generate secondary pollution. Furthermore, small pores cannot sustain microbes, which rely on the surface roughness [18]. Yeboah et al. [2] compared the characteristics of fly ash from power plants, ash from the co-combustion of coal with biomass, and biomass ash, which found that biomass ash could be used as the water-treatment filler and biofilm carrier material due to its smaller specific gravity, wider distribution of particle sizes, higher content of unburned carbon, and larger specific surface area. The surface properties of the support material are generally optimized by an acid-organic composite (sucrose–phosphoric acid, sodium alginate–phosphoric acid, and polyethylene glycol–phosphoric acid) modification treatment through a modification procedure: soaking in acid solution, surface corrosion, functional group modification [19,20]. Among these, sodium alginate–phosphoric acid combined modification had the best specific surface area and the lowest cost of batch modification treatment [21]. Therefore, in this paper, biomass power plant ash with the right amount of phosphoric acid and sodium alginate was selected in order to make the new modified biofilm carrier material. Based on the performance analyses before and after modification of the biomass ash material, combining with a biofilm formation experiment and high-flux 16S rDNA sequencing, the feasibility of efficient utilization of biomass power plant ash as a microbial carrier in water treatment is verified.

2. Materials and methods

2.1. Source and leaching of biomass ash

Biomass ash materials were provided by Kaidi Green Energy Development Co., Ltd. in Huoqiu County, Anhui Province of China. The density of the biomass power plant ash is 2.10 g mL^{-1}. After the removal of impurities, screening, and washing, biomass ash with particle sizes ranging from 0.5 to 1.0 mm was regarded as the raw materials. Since biomass ash may contain harmful elements [22], its safety was evaluated before modification. The HJ/T299-2007, Solid Waste-extraction Procedure for Leaching Toxicity –Sulphuric Acid & Nitric Acid Method[S] was used for the heavy metal toxicity leaching experiment. The concentration of Cu, Zn, As, Cd, Pb, Cr, and Hg in the leaching liquid was determined by inductively coupled plasma mass spectrometry (ICP, NexION 300X, PerkinElmer Enterprise Management Co., Ltd, Shanghai). The contents of metals in all tested samples were less than the detection limit and were far lower than the standard values provided by the Identification Standards for Hazardous Wastes Identification for Extraction Toxicity GB5085.3-2007[S], which indicated that the biomass ash has no ecological risk itself as the water-treatment filler.

2.2. Modification of the biofilm carrier

Pre-treated biomass ash (0.5 kg) was added to a solution of 1 L water with 3.5 g sodium alginate and 170 mL phosphoric acid, and mixed for 1 h. The mixture was aged at room temperature for 24 h and then filtered and dried to recover the biomass ash.

2.3. Characterization of ash before and after modification

The specific surface area and pore size distribution of biomass ash before and after modification were determined by BET (Brunauer–Emmett–Teller, 3H-2000PS4, Bestech Instrument Technology Co. Ltd., Beijing). The composition of the functional groups was tested using a Fourier transform infrared spectrometer (FT-IR, Avatar 360, Nicolet) and processed by using a KBr pellet. SEM with energy dispersive X-ray (SEM-EDX, JMS-35 CF Type, JEOL Co. Ltd., Beijing) was used for the surface morphology observations and elemental analysis of biomass ash.

2.4. Biofilm formation test

Raw biomass ash materials (5 g) and biomass ash after modification (5 g) were added to 250 mL conical flasks. Activated sludge (60 mL), taken from the aerobic pool of Quyang Wastewater Treatment Plant in Shanghai was inoculated into each conical flask. The solution was mixed thoroughly and left to stand for 1 h and then the supernatant was removed. Subsequently, experimental water (200 mL, prepared by inferior V channel water and ammonium chloride, including 25.6 mg L^{-1} of chemical oxygen demand (COD_{cr}) and 19.8 mg L^{-1} of NH_3–N) was added into each conical flask. The conical flasks were put into a constant temperature oscillating box for testing at room temperature. The contents of COD_{cr} and NH_3–N in the supernatant were determined every day to verify the treatment effect. After continuous observation for 7 d, the modified biomass ash after biofilm formation was removed for freezing and dying. The samples were then analyzed by SEM to observe their morphology and structure.

2.5. High-flux 16S rDNA sequencing

The biofilm carrier flora after biofilm formation for 7 d was determined by the 454 high-flux sequencing method. The microbial diversity of the genomic DNA of the samples was detected by 1% agarose gel electrophoresis. The primers for polymerase chain reaction (PCR) were 338F: ACTCCTACGGGAGGCAGCAG and 806R: GGACTACHVGGGTWTCTAAT. The reaction system was

TransGen AP221-02: TransStart Fastpfu DNA Polymerase, 20 μL reaction system. PCR products were detected by 2% agarose gel electrophoresis. Based on the preliminary results of the electrophoresis, PCR products were quantified and homogeneously mixed by a Picogreen dye fluorescence meter. Finally, high-flux sequencing was carried out on the amplification products using the high-flux sequencing platform Illumina Miseq PE300 of Shanghai Majorbio Bio-Pharm Technology Co. Ltd.

3. Results and discussion

3.1. Element analysis of biomass ash

The EDX element analysis results of the raw materials of biomass power plant ash are shown in Fig. 1. The elements in raw biomass power plant ash were composed of C, O, Si, Ca, Na, Mg, Al, P, K, and Fe, of which C, O, and Si accounted for large proportions (16.36%, 34.30%, and 26.73%, respectively). The elemental composition of biomass power plant ash is different from fly ash. The carbon content in biomass power plant ash was as high as 16.36%, which is more conducive to increasing the surface roughness and specific surface area of ash in the acid modification process [23].

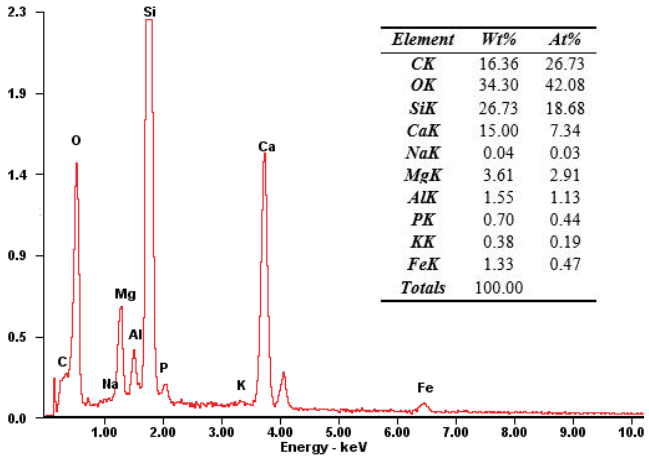

Element	Wt%	At%
CK	16.36	26.73
OK	34.30	42.08
SiK	26.73	18.68
CaK	15.00	7.34
NaK	0.04	0.03
MgK	3.61	2.91
AlK	1.55	1.13
PK	0.70	0.44
KK	0.38	0.19
FeK	1.33	0.47
Totals	100.00	

Fig. 1. Element analysis of biomass ash.

3.2. Performance analysis before and after modification

The external morphology structures of biomass ash before and after modification are shown in Fig. 2. After modification, the surface of the biomass ash is more rough, and the porous honeycomb structure is more remarkable. Biomass ash contains many carbon residues which is similar to activated carbon, so its surface becomes rougher after acid dipping, which can increase its specific surface area and the physical adsorption capacity [23].

3.2.1. BET analysis

The results of BET analysis of biomass ash before and after modification are shown in Table 1. Both the specific surface area and the average pore volume of biomass ash were increased after modification. The specific surface area after modification was about sevenfold greater and the average pore volume was twofold larger than that of the initial ash material. The pore size of the raw biomass ash before modification was in the range of 3.5–4.3 and 30.3–33.1 nm. After modification, the pore sizes were reduced to 3.5–4.2 and 14.8–17.5 nm. The pore size distribution range indicates that the majority of pores of the biomass ash before modification were mesoporous. The decrease in the pore sizes of modified biomass ash was due to the effect of phosphate, which is similar to the modification of fly ash. Yang et al. [24] found that the pore size of fly ash after acid modification was reduced and the specific surface area increased when using the acid method to modify fly ash [24]. The complex or high molecular polymer was generated due to the oxidizing reaction of phosphoric acid with SiO_2 and Al_2O_3 in biomass ash, which changed the pore structure of the material. At the same time, the generated compound could play a bridging role in the adsorption process, which is helpful for suspended particle adsorption, flocculation and precipitation [25,26]. The increase in the specific surface area of modified biomass ash would increase its adsorption performance and provide more microbial attachment sites for microbial carrier.

The adsorption isotherm is the basic parameter to study the surface and pores of the material. The shape of the adsorption–desorption curve can reflect the pore structure of the material [27]. The adsorption isotherms of biomass

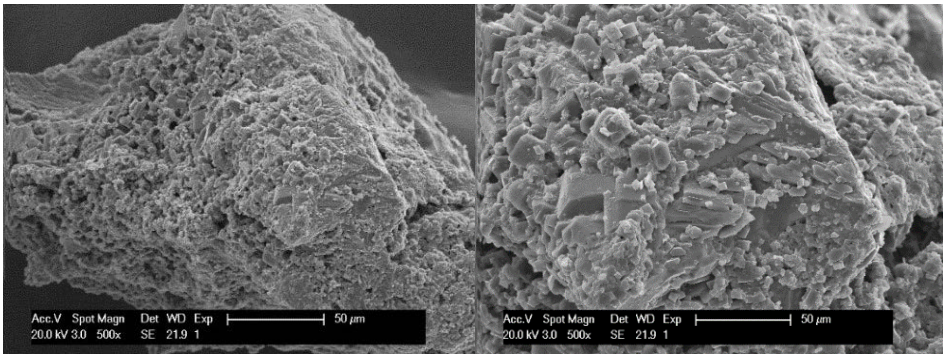

(a) (b)

Fig. 2. SEM of biomass ash before and after modification ((a) and (b) reflected raw biomass ash and modified biomass ash, respectively).

Table 1
Results of BET analysis of biomass ash before and after modification

Sample	Specific surface area ($m^2 g^{-1}$)	Average pore volume ($cm^3 g^{-1}$)	Pore size distribution (nm)
Raw biomass ash	2.22	0.0492	3.5–4.3 nm, 30.3–33.1 nm
Modified biomass ash	15.1	0.0984	3.5–4.2 nm, 14.8–17.5 nm

ash before and after modification showed a similar trend (Fig. 3). According to the classification of IUPAC, the adsorption isotherm of modified biomass ash showed an inverse S shape, which is similar to the type IV isotherm. When the relative pressure was low, the adsorption isotherm showed a dome shape and rose slightly, which was due to the monolayer adsorption on the surface of the modified biomass ash. However, when the inflection point of the adsorption isotherm was low, the saturated adsorption amount of the monolayer of the modified biomass ash was low. With the increasing relative pressure, the adsorption isotherm was approximately linear. Multilayer adsorption occurred on the modified biomass ash. When the relative pressure was high, the pores were concentrated on the surface of the modified biomass ash. The isotherm rose sharply, and the adsorption and desorption isotherms did not overlap and thus formed an H3-type hysteresis loop. These data indicate that the modified biomass ash had open air-permeable cylindrical and parallel panel holes [28]. The type IV adsorption isotherm and the H3-type hysteresis loop show that the majority of pores of the modified biomass ash were mesoporous. When the relative pressure was close to the saturated vapour pressure, the adsorption did not show a horizontal line, which indicates that there were large pores.

3.2.2. Fourier transform infrared spectra analysis

The FT-IR spectra of biomass ash before and after modification are shown in Fig. 4. The number of surface functional groups of the raw biomass ash materials was small. The adsorption peak at 456–1,051 cm^{-1} were Si–O, Si–Si keys, in

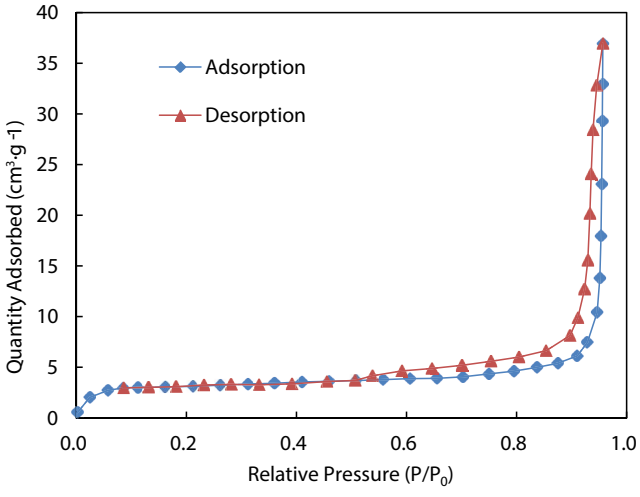

Fig. 3. Adsorption and desorption curves of modified biomass ash.

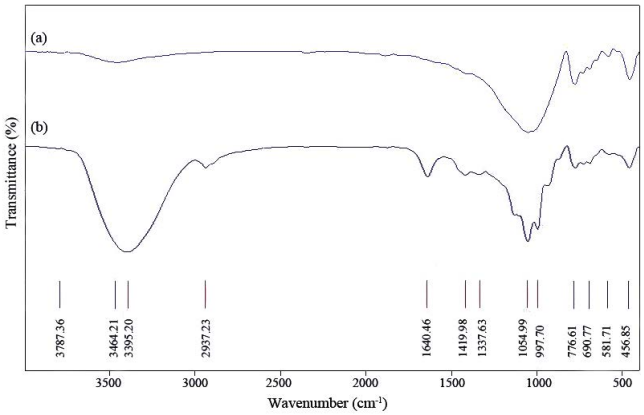

Fig. 4. FT-IR of biomass ash before and after modification ((a) and (b) reflected raw biomass ash and modified biomass ash, respectively).

which the stretching vibration of Si–O–Si was seen at about 1,050 cm^{-1}. After the modification of biomass ash by sodium alginate/phosphoric acid, the number of surface functional groups increased. The adsorption peak at about 3,400 cm^{-1} was enhanced and the peak shape was wide, which indicates that there were hydroxyl groups of alcohol or phenol in the modified biomass ash [29]. The weak adsorption peak at about 2,900 cm^{-1} was C–H keys [30]. The weak absorption peaks at 1,640 and 1,419 cm^{-1} were the stretching vibrations of carboxylate groups [31]. Two strong adsorption peaks at 1,054.99 and 997.7 cm^{-1} were the stretching vibrations of phosphate and hydrogen phosphate groups, respectively [32]. The appearance of carboxylate groups in the modified biomass ash shows that there was a strong electrostatic interaction between the biomass ash and the carboxylate groups in the sodium alginate molecular chain [33]. Sodium alginate had a good biofilm formation impact on the surface of biomass ash, which enriched the surface functional groups of biomass ash. The appearance of phosphate and hydrogen phosphate suggested that the oxide reaction of phosphate with Al_2O_3 and other oxides in the biomass ash promoted the generation of the complex or polymer. The biomass ash was similar to activated carbon in adsorption principle. The adsorption was mainly determined by the physical properties, including the specific surface area and surface functional groups, in which specific surface area and pore structure affect the adsorption capacity of biomass ash, and the oxygen-containing functional groups affected the interaction between adsorbates [34]. The increase in oxygen-containing functional groups in modified biomass ash was beneficial for adsorption of water molecules, heavy metal ions, and organic compounds. In particular, with carbonyl as the electron donor, the adsorption ability of organic matters was enhanced [35]. As the

microbial carrier, the organic matter and other nutrients adsorbed by the modified biomass ash were more conducive to the growth of microorganisms.

3.3. Biofilm formation of carrier materials

3.3.1. Biofilm formation effect

The external morphology of biofilm formation of the modified biomass ash is shown in Fig. 5. The biofilm was attached to the surface of the biomass ash, which made the surface of the material more compact, and the modified biomass ash was good. Modified biomass ash showed a good biofilm formation effect.

3.3.2. Effect of biofilm formation on water treatment

In the experiments of biofilm formation of biomass ash before and after modification, the concentration changes of COD_{cr} and NH_3–N in the overlying water are shown in Fig. 6. The concentrations of COD_{cr} and NH_3–N in the two groups changed a little on day 2 and began to sharply decrease after 3 d of experiment. These results indicated that the biofilm gradually formed on the surface of the materials. The raw biomass ash materials showed a good removal effect on COD_{cr}. Its removal rate reached to 47.1% on day 7. Its removal effect on NH_3–N tended to be stable after 4 d with a removal rate of 35.2%. The modified biomass ash had a better removal effect on COD_{cr} and NH_3–N than that of raw ash materials, of which its removal rates reached to 67.6% for COD_{cr} and 65.7% for NH_3–N on day 7. However, there was no stable trend, which suggested that the biomass ash was a better microbial carrier after modification by sodium alginate–phosphoric acid.

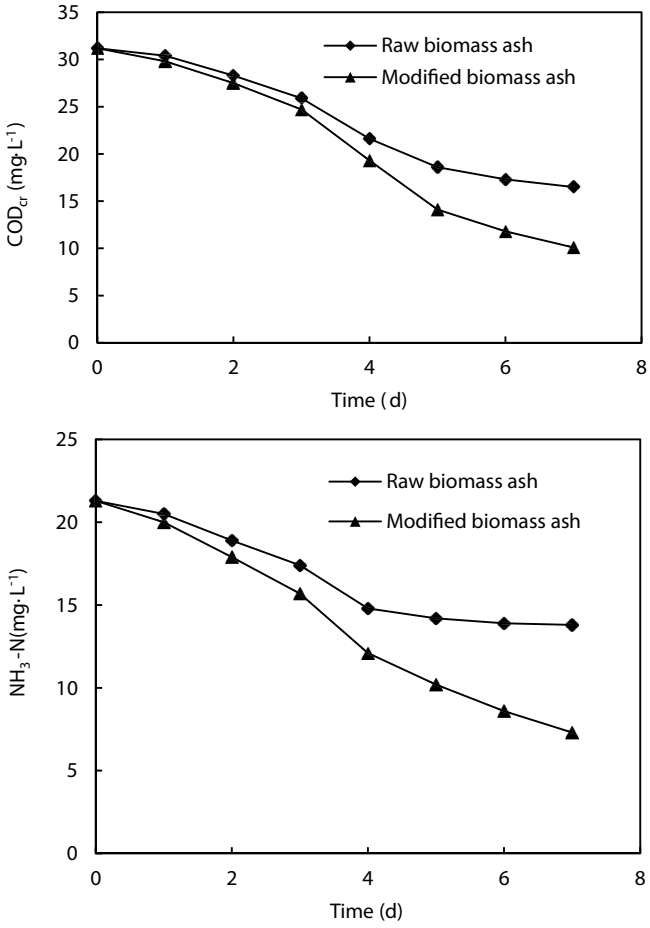

Fig. 6. Concentration changes of COD_{cr} and NH_3–N in test water.

3.3.3. Analysis of microbial diversity and taxonomy

High-flux sequencing was carried out on the biofilm carrier material after biofilm formation for 7 d. The number of valid sequences was 67,291 with an average length of 443.44 bp after impurity removal. These sequences were categorized into 898 operational taxonomic units (OTU). OTU classification was carried out on all sequences at the 97% similarity level, and then the diversity index and the taxonomy of the community structure were analyzed. The rarefaction curve of the sample is shown in Fig. 7. When the number of sequences was greater than 40,000, new OUT could be detected, which indicates that high-flux sequencing could obtain abundant biological information. At the same time, the rarefaction curve tended to be flat with increasing numbers of sequences, which indicates that the sequencing was appropriate.

At the phylum level, the bacterial phyla with a relative abundance of less than 1% were merged into others. The bacterial community distribution of the biofilm with a similarity of 97% is shown in Fig. 8. The main microbial communities were Proteobacteria, Bacteroidetes, Acidobacteria, Nitrospirae,

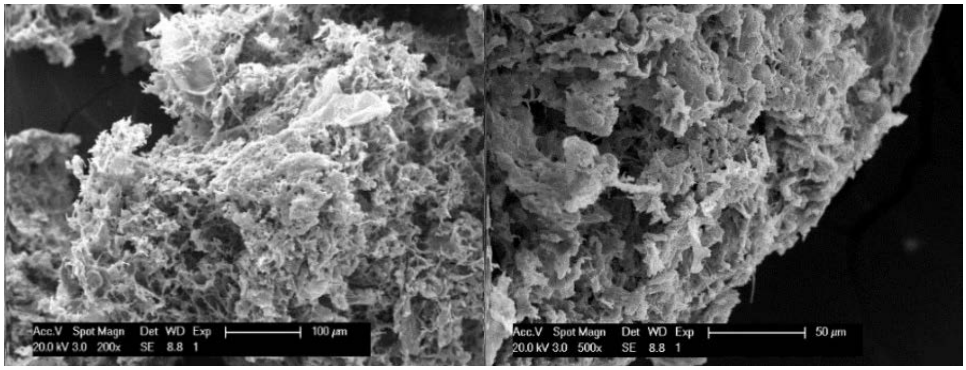

Fig. 5. SEM of modified biomass ash after biofilm formation.

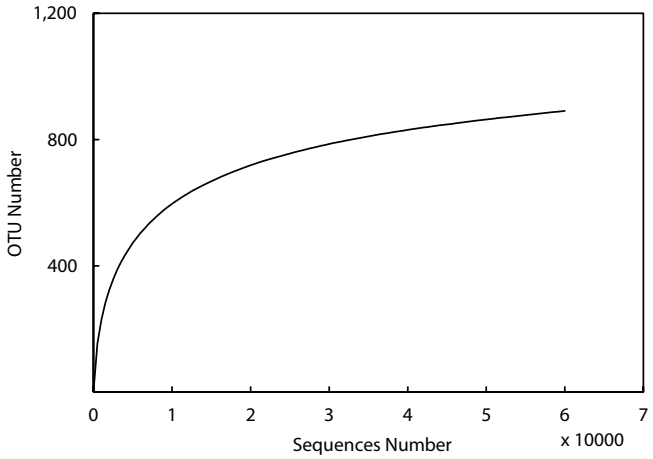

Fig. 7. Rarefaction curve of the microbial carrier sample.

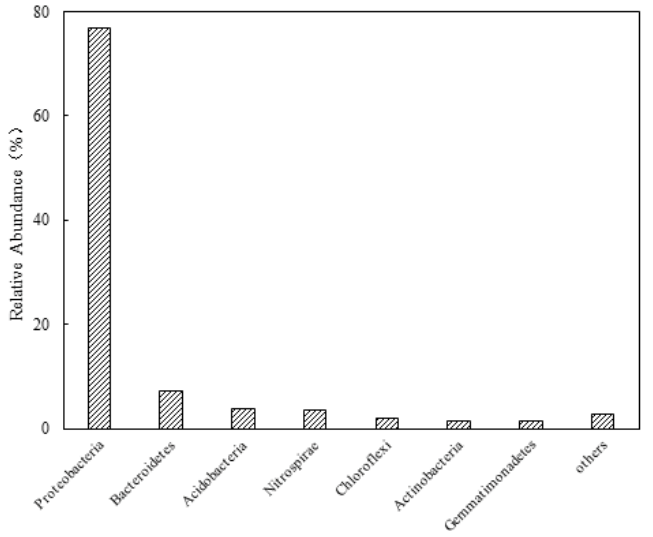

Fig. 8. Bacterial communities at the phylum level of the microbial carrier sample.

Chloroflexi, Actinobacteria and Gemmatimonadetes, of which Proteobacteria accounted for the largest proportion of 77.09%, followed by Bacteroidetes (7.43%), Acidobacteria (3.99%), and Nitrospirae (3.69%).

Proteobacteria was the largest phylum in bacteria, in which β-proteobacteria accounted for 25.7% in biofilms. β-Proteobacteria can decompose organic matters under anaerobic conditions to absorb nutrients and can make use of ammonia and volatile fatty acids. They are associated with denitrification [36]. Teira et al. [37] found that the nitrification rate has a significant positive linear correlation with the growth rate of β-proteobacteria. The second highest proportion of bacteria in biofilms was Bacteroidetes. *Flavobacterium* and other anaerobic bacteria can use the organic matter in the environment for heterotrophic nitrate reduction [38]. Acidobacteria is a kind of acidophilic bacteria that play an important role in the soil ecosystem and have been found on many biofilms, but their main function need more studies [39,40]. Nitrospirae is a kind of gram-negative bacteria, of which Nitrospirae is an important nitrite-oxidising bacteria [41,42].

4. Conclusion

In this study, we developed a new biofilm carrier by using biomass power plant ash modified by a combination of sodium alginate and phosphoric acid. After modification, the specific surface area of the biomass ash was sevenfold larger and the average pore volume was twofold greater than those of the raw material. The average pore size of modified biomass ash was reduced. Modified biomass ash and its raw material had open air-permeable cylindrical and parallel panel pores, of which mainly were mesoporous. Furthermore, the modification also increased the amount of surface functional groups, including hydroxyl, carboxyl, phosphate and hydrogen phosphate groups, and C–H keys.

In the biofilm formation process, the modified biomass ash had a better removal effect on COD_{cr} and NH_3–N (67.6% and 65.7%, respectively). The biofilm was attached to the surface of the material after formation that made the structure more compact. The growth effect of the biofilm was good. The high-flux sequencing of the biofilm carrier showed that Proteobacteria, which are associated with nitrification and denitrification, accounted for the largest proportion in the main microbial communities (77.09%) followed by Bacteroidetes (7.43%), Acidobacteria (3.99%), and Nitrospirae (3.69%), which are related to heterotrophic nitrate reduction. These results are consistent with the good removal effect on COD_{cr} and NH_3–N.

Acknowledgements

This work was supported by National Natural Science Foundation of China (No. 51679140) and the training and funding plan for young teachers in Universities in Shanghai.

References

[1] G.L. Wang, L.H. Shen, C.D. Sheng, Characterization of biomass ashes from power plants firing agricultural residues, Energy Fuels, 26 (2012) 102–111.
[2] N.N.N. Yeboah, C.R. Shearer, S.E. Burns, K.E. Kurtis, Characterization of biomass and high carbon content coal ash for productive reuse applications, Fuel, 116 (2014) 438–447.
[3] S. Wang, L. Baxter, F. Fonseca, Biomass fly ash in concrete: SEM, EDX and ESEM analysis, Fuel, 87 (2008) 372–379.
[4] J. Rosales, M. Cabrera, M.G. Beltrán, M. López, F. Agrela, Effects of treatments on biomass bottom ash applied to the manufacture of cement mortars, J. Cleaner Prod., 54 (2017) 424–435.
[5] N.C. Cruz, S.M. Rodrigues, L. Carvalho, A.C. Duarte, E. Pereira, P.F.A.M. Römkens, L.A.C. Tarelho, Ashes from fluidized bed combustion of residual forest biomass: recycling to soil as a viable management option, Environ. Sci. Pollut. Res., 24 (2017) 14770–14781.
[6] M. Quirantes, F. Calvo, E. Romero, R. Nogales, Soil-nutrient availability affected by different biomass-ash applications, J. Soil Sci. Plant Nutr., 16 (2016) 159–163.
[7] J.P. Ribeiro, E.D. Vicente, A.P. Gomes, M.I. Nunes, C. Alves, T. Lac, Effect of industrial and domestic ash from biomass combustion, and spent coffee grounds, on soil fertility and plant growth: experiments at field conditions, Environ. Sci. Pollut. Res., 24 (2017) 1–8.
[8] S. Zelazny, V. Cablik, L. Cablikova, Attempts to obtain potassium and phosphorus from fly ash from biomass, Przem. Chem., 94 (2015) 956–959.

[9] Zhongying Changjiang International New Energy Investment Co. Ltd. Method for Producing Nano Silicon Dioxide and Nano Calcium Carbonate by Using Rice Hull Ash and Flue Gas of Biomass Power Plant [P/OL], CN 103693650 B, 2015–11–18 (In Chinese with English Abstract).
[10] S. Nethaji, A. Sivasamy, R.V. Kumar, A.B. Mandal, Preparation of char from lotus seed biomass and the exploration of its dye removal capacity through batch and column adsorption studies, Environ. Sci. Pollut. Res., 20 (2013) 3670–3678.
[11] L. Xu, X. Zheng, H. Cui, J. Liang, Z. Tao, Z. Zhu, B. Liu, J. Zhou, Adsorption of Cu^{2+} in water by biomass ash, Environ. Chem., 35 (2016) 1642–1648. (In Chinese with English abstract)
[12] U. Vaid, S. Mittal, J.N. Babu, Removal of hexavalent chromium from aqueous solution using biomass derived fly ash from waste-to-energy power plant, Desal. Wat. Treat., 52 (2014) 7845–7855.
[13] D. Tian, M. Gao, K. Wang, Experimental research on the treatment of life sewage by biomass ash particle size, J. Soil Water Conserv., 29 (2015) 218–222. (In Chinese with English abstract)
[14] Y. Bao, G. Dai, Time-gradient nitric acid modification of CF biofilm-carrier and surface nature effects on microorganism Immobilization behavior in wastewater, Biotechnol. Biotechnol. Equip., 27 (2013) 3918–3922.
[15] S. Xiong, L. Guan, Z. Jin, A. Wang, Wastewater treatment by biofilter with composite fly ash filter material as main media, Environ. Sci. Technol., 35 (2012) 138–140. (In Chinese with English abstract)
[16] X. Ji, F. Wang, H. Zhang, L. Gu, L. Wu, The application status que and development direction of bio-carrier in water treatment technology, Technol. Water Treat., 35 (2009) 9–13. (In Chinese with English abstract)
[17] W. Ding, X. Zeng, Y. Wang, Y. Du, Q. Zhu, Characteristics and performances of biofilm carrier prepared from agro-based biochar, China Environ. Sci., 31 (2011) 1451–1455. (In Chinese with English abstract)
[18] J. Cao, G. Zhang, Z. Mao, Z. Fang, B. Han, Immobilization of sulfate reducing bacteria, Chin. J. Process Eng., 7 (2007) 1009–1013. (In Chinese with English abstract)
[19] H.B. Peng, P. Gao, G. Chu, Enhanced adsorption of Cu(II) and Cd(II) by phosphoric acid-modified biochars, Environ. Pollut., 229 (2017) 846–853.
[20] B.K.S. Khanal, B. Bhandari, S. Prakash, D.S. Liu, P. Zhou, N. Bansal, Modifying textural and microstructural properties of low fat Cheddar cheese using sodium alginate, Food Hydrocolloids, 83 (2018) 97–108.
[21] Y. Jia, Application of Biomass Power Plant Bottom Ash in Water Treatment [D], University of Shanghai for Science and Technology, Shanghai 200093, China, 2018.03 (In Chinese with English Abstract).
[22] I. Obernberger, K. Supancic, Possibilities of Ash Utilization From Biomass Combustion Plants, Proceedings of the 17th European Biomass Conference and Exhibition; Hamburg, Germany, June 29–July 3, 2009.
[23] K. Xu, T. Deng, J. Liu, W. Peng, Study on the phosphate removal from aqueous solution using modified fly ash, Fuel, 89 (2010) 3668–3674.
[24] W. Yang, W. Zhong, X. Jiang, Study on the adsorption of the chroma in wastewater by modified fly ash, Ind. Saf. Environ. Prot., 36 (2010) 7–8. (In Chinese with English abstract)
[25] P. Ouyang, H. Fan, X. Zhang, L. Chen, Research progress of the modification mechanism of fly ash based on adsorption, J. Mater. Sci. Eng., 32 (2014) 619–624. (In Chinese with English abstract)
[26] Y. Bai, A. Zhang, J. Zhou, Study on treatment of methylene blue wastewater by fly ash adsorption-fenton and thermal regeneration, Chin. J. Environ. Sci., 33 (2012) 2419–2426. (In Chinese with English abstract)
[27] X. Wei, R. Liu, T. Zhang, X. Liang, Micro-pores structure characteristics and development control factors of shale gas reservoir: a case of Longmaxi formation in XX area of southern Sichuan and northern Guizhou, J. Nat. Gas Geosci., 24 (2013) 1048–1059. (In Chinese with English abstract)
[28] P. Chen, X. Tang, The research on the adsorption of nitrogen in low temperature and micro-pore properties in coal, J. China Coal Soc., 26 (2001) 552–556. (In Chinese with English abstract)
[29] Y. Zhen, F. Li, L. Ge, Y. Guo, Spectral analysis of modified kaolinite filled with polypropylene, Spectrosc. Spectral Anal., 31 (2011) 3036–3039. (In Chinese with English abstract)
[30] J. Yan, H. Zhao, J. Wang, F. Qiu, D. Yang, Preparation a composite of graphene/diisocyanate/β-cyclodextrin and its application to determination of Cu (II), Phys. Testing Chem. Anal. Part B: Chem. Anal., 51 (2015) 1302–1306. (In Chinese with English abstract)
[31] H. Liu, Q. Guo, M. Xue, X. Rong, J. Liu, X. Yang, Effect of oxidation degree on tribological properties of graphite oxide modified epoxy resin coatings, Phys. Testing Chem. Anal. Part A: Phys. Testing, 49 (2013) 727–730. (In Chinese with English abstract)
[32] W. Wang, R. Hao, X. Zhang, J. Wan, L. Zhong, Preparation and phosphorus removal mechanism of highly efficient phosphorus adsorbent Mg/Al-LDO, Chin. J. Environ. Sci., 38 (2017) 572–579. (In Chinese with English abstract)
[33] L. Li, B. Liu, B. Han, L. Tang, Preparation and bioactivities of sodium alginate/chitosan microcarriers, Appl. Chem. Ind., 42 (2013) 233–238. (In Chinese with English abstract)
[34] Y. Yang, L. Li, Z. Sun, L. Du, The research on the surface oxidation modification of activated carbon and its adsorption mechanisms of organic matter and heavy metal ions, Sci. Technol. Eng., 12 (2012) 6132–6138. (In Chinese with English abstract)
[35] G. Meng, A. Li, Q. Zhang, Studies on the oxygen-containing groups of activated carbon and their effects on the adsorption character, Ion Exch. Adsorpt., 23 (2007) 88–94. (In Chinese with English abstract)
[36] T.R. Thomsen, Y. Kong, P.H. Nielsen, Ecophysiology of abundant denitrifying bacteria in activated sludge, FEMS Microbiol. Ecol., 60 (2007) 370–382.
[37] E. Teira, S. Martinez-Garcia, C. Lonborg, X.A. Alvarez-Salgado, Betaproteobacteria growth and nitrification rates during long-term natural dissolved organic matter decomposition experiments, Aquat. Microb. Ecol., 63 (2011) 19–27.
[38] C.M. Falkentoft, E. Müller, P. Arnz, P. Harremoës, H. Mosbaek, P.A. Wilderer, Population changes in a biofilm reactor for phosphorus removal as evidenced by the use of FISH, Water Res., 36 (2002) 491–500.
[39] B.U. Foesel, V. Nägele, A. Naether, P.K. Wüst, J. Weinert, M. Bonkowski, Determinants of Acidobacteria activity inferred from the relative abundances of 16S rRNA transcripts in German grassland and forest soils, Environ. Microbiol., 16 (2014) 658–675.
[40] Q. Ma, M. Gao, W. Tan, H. Xie, W. Wang, Role of new type floating island in improving effluent quality and the characterization of microbe on biofilm carrier, Environ. Sci., 32 (2011) 1596–1601. (In Chinese with English abstract)
[41] F. Maixner, D.R. Noguera, B. Anneser, H. Daims, Nitrite concentration influences the population structure of Nitrospira-like bacteria, Environ. Microbiol., 8 (2006) 1487–95.
[42] H.W. Lee, S.Y. Lee, J.W. Lee, J.B. Park, E.S. Choi, K.P. Yong, Molecular characterization of microbial community in nitrate-removing activated sludge, FEMS Microbiol. Ecol., 41 (2002) 85–94.